

Photonic Topological Insulator: An Introduction

Niranjay K R^{*} and Pritish Karmakar[†]
Department of Physical Sciences, IISER Kolkata

(Dated: January 3, 2025)

This paper introduces photonic topological insulators (PTIs), drawing parallels with electronic systems like the Integer and Quantum Spin Hall Effects. Key concepts include the Berry phase, Chern number, and bulk-edge correspondence. We explore the translation of topology to photonic systems, highlight experimental realizations, and discuss potential applications of PTIs.

I. INTRODUCTION

In this term paper we would like to introduce photonic topological insulators and draw parallels with topological insulators. Topological insulators (TIs) are a class of materials that have revolutionized our understanding of condensed matter physics. These systems exhibit a unique duality: while their bulk is insulating, their edges or surfaces host conducting states that are robust against disorder and defects. This phenomenon is rooted in the system's topology, a branch of mathematics that characterizes global properties of systems insensitive to small perturbations. The quantum Hall effect (QHE) serves as the archetypal example, where the breaking of time-reversal symmetry (TRS) by a magnetic field results in edge states protected by the quantized Chern number, a topological invariant.

Recently, the concepts underlying TIs have transcended condensed matter physics and found exciting applications in photonics, leading to the advent of photonic topological insulators (PTIs). These systems mimic the behaviour of electronic TIs but operate with light instead of electrons. Unlike traditional photonic materials, PTIs can support unidirectional edge modes that are immune to backscattering, even in the presence of imperfections or disorders. This property holds immense potential for applications in photonic circuits, robust signal transmission, and quantum technologies.

In PTIs, time-reversal symmetry breaking is typically achieved using gyromagnetic materials in the presence of an external magnetic field. These materials exhibit magneto-optical effects, creating asymmetric propagation of light that mirrors the behaviour of electrons in the QHE. The gyromagnetic response enables the formation of one-way edge states analogous to those in electronic TIs, but without requiring a Fermi surface or electronic charge.

This paper introduces the fundamental principles of topological insulators and their extension to photonic systems, known as photonic topological insulators (PTIs). It begins by reviewing Bloch's theorem and its application in both electric and photonic systems. Fur-

ther, we emphasize the importance of the topology in band theory and the calculation of the Chern no. We later transition to the quantum Hall effect (QHE) as a foundational concept, including the generation of Landau levels, edge state formation, and their contribution to quantized conductivity. The discussion highlights the role of the Chern number as a topological invariant and provides an overview of the mathematical framework for its calculation.

The transition to PTIs emphasizes key differences between electronic and photonic systems. Unlike electrons, photons are charge-neutral and lack intrinsic non-reciprocity, requiring gyromagnetic materials to break time-reversal symmetry (TRS) and achieve non-trivial topological phases. These differences, alongside the unique properties of photons, are explored to illustrate how photonic systems can realize analogues of QHE-like behaviour.

Before delving into PTIs, the paper introduces topological insulators more broadly. These materials exhibit edge states that are protected by topology. In electronic systems, these states are helical and TRS-protected, forming counterpropagating channels immune to non-magnetic scattering. In QHE systems, edge states arise from TRS breaking and the non-trivial topology of the bulk, which leads to robust, unidirectional edge modes.

Building on the understanding of QHE, the paper gives a brief overview of the quantum spin Hall effect (QSHE), where TRS is preserved. This transition sets the stage for PTIs, which extend these principles to photonic systems. The mathematical framework underlying Chern PTIs, including the calculation of the Chern number, is briefly outlined, showing how photonic band structures exhibit topologically protected states. The role of gyromagnetic materials in creating anisotropic permeability and breaking TRS in photonic systems is also discussed.

Finally, the significance of PTIs in modern photonics is highlighted, with potential applications ranging from robust optical communication to enhanced light manipulation. The comparison between Chern PTIs (analogous to QHE) and valley PTIs introduces a broader context for topological photonics.

This framework will allow us to establish the connection between these various topological phenomena, setting the stage for a more detailed exploration of their ap-

^{*} Roll no: 21MS162, email: nkr21ms162@iiserkol.ac.in

[†] Roll no: 21MS179, email: pk21ms179@iiserkol.ac.in

plications and implications in photonics and beyond. By combining insights from condensed matter physics and photonics, PTIs exemplify the cross-disciplinary nature of topological science, paving the way for a deeper understanding of light-matter interactions in structured materials.

II. SOME BASIC CONCEPTS

Before proceeding with this topic in detail, we will discuss some basic concepts necessary to understand the later section.

A. Berry phase and Chern number

We talk about the Berry phase in the context of a quantum system when the Hamiltonian of the system depends on some adiabatically varying parameter. When the state of the system varies adiabatically with the parameters on which it depends, other than the dynamical phase, an additional geometric phase arises, which we call the Berry phase. The Berry phase depends only on the geometry or path it takes in the parameter space. Consider a system driven by the Hamiltonian H that depends on the parameter \mathbf{k} which is varying in \mathbf{k} -space. The eigenvalue equation is as follows:

$$H(\mathbf{k}) |\psi_n(\mathbf{k})\rangle = E_n(\mathbf{k}) |\psi_n(\mathbf{k})\rangle. \quad (1)$$

The parameter \mathbf{k} varies ‘adiabatically’ so that there is no crossover between the two states of the system. The *Berry connection* (or *Berry vector potential*) for the n^{th} state is defined as

$$\mathbf{A}_n(\mathbf{k}) = i \langle \psi_n(\mathbf{k}) | \nabla_{\mathbf{k}} | \psi_n(\mathbf{k}) \rangle \quad (2)$$

and the Berry curvature is defined as

$$\gamma_n = \int_l d\mathbf{k} \cdot \mathbf{A}_n(\mathbf{k}) \quad (3)$$

where l is the smooth curve traced by the evolution of the parameter \mathbf{k} in \mathbf{k} -space. The *Berry curvature* is defined as

$$\Omega_n(\mathbf{k}) = \nabla_{\mathbf{k}} \times \mathbf{A}_n(\mathbf{k}) \quad (4)$$

We mostly evaluate the Berry phase over a smooth closed loop. By using Stokes’s theorem, we can write the Berry phase as

$$\gamma_n = \oint_l d\mathbf{k} \cdot \mathbf{A}_n(\mathbf{k}) = \iint_s d\mathbf{S} \cdot \Omega_n(\mathbf{k}) \quad (5)$$

where s be the surface enclosed by the loop l and $d\mathbf{S}$ be the differential surface element over surface s . We define the Chern number as

$$C_n = \frac{1}{\pi} \iint_s d\mathbf{S} \cdot \Omega_n(\mathbf{k}) \quad (6)$$

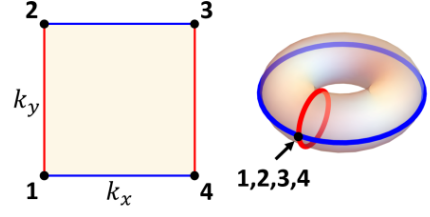


FIG. 1. The 2D BZ is equivalent to the Torus, thanks to the periodic gauge choice of $u_{n,\mathbf{k}}(\mathbf{x})$, which results in periodicity of $|\psi_{n,\mathbf{k}}\rangle$ over \mathbf{k} in momentum space (BZ). (taken from [4])

One can note that under local gauge transformation on the state of the system i.e., $|\psi_n(\mathbf{k})\rangle \rightarrow e^{i\chi(\mathbf{k})} |\psi_n(\mathbf{k})\rangle$, the Berry phase is equal up to modulo 2π due to the single valuedness of $e^{i\chi(\mathbf{k})}$. The Berry curvature and Chern number are invariant under such transformation.

B. Band theory in lattice

The concept of band structure in a 2D periodic lattice is essential for the discussion of the topology of 2D photonic crystal. For an electronic system in a periodic potential, the Hamiltonian $H(\mathbf{x}, \mathbf{p})$ will obey spatial periodic condition i.e., $H(\mathbf{x} + \mathbf{a}_i, \mathbf{p}) = H(\mathbf{x}, \mathbf{p})$, where $\{\mathbf{a}_i\}$ are the lattice vectors. By the Bloch’s theorem, due to the translational invariance of the system, the eigenstate of the system is given by

$$\psi_{n,\mathbf{k}}(\mathbf{x}) = e^{i\mathbf{k} \cdot \mathbf{x}} u_{n,\mathbf{k}}(\mathbf{x}). \quad (7)$$

where n is the band index, \mathbf{k} is the crystal momentum in the 1st Brillouin zone (BZ) and the function $u_{n,\mathbf{k}}(\mathbf{x})$ is periodic as the Hamiltonian. The eigenvalue equation of this Hamiltonian is

$$H |\psi_{n,\mathbf{k}}\rangle = E_{n,\mathbf{k}} |\psi_{n,\mathbf{k}}\rangle \quad (8)$$

For 1D periodic lattice, the 1st BZ is $[-\pi/a, \pi/a)$ where a is the periodicity of the crystal. For a 2D square lattice, it is $[-\pi/a, \pi/a) \otimes [-\pi/a, \pi/a)$ where a be the periodicity of the crystal in both x and y direction. Let $\{\mathbf{b}_i\}$ are the reciprocal lattice vector, then any momentum \mathbf{q} not in 1st BZ can be written as $\mathbf{q} = \mathbf{k} + \mathbf{b}$, for \mathbf{k} in 1st BZ and \mathbf{b} is a reciprocal lattice vector. Taking periodic gauge choice of $u_{n,\mathbf{k}}(\mathbf{x})$ such that $|\psi_{n,\mathbf{q}}\rangle = |\psi_{n,\mathbf{k}}\rangle$, we can think the 1st BZ, in 1D case, is a ring and in 2D case, its a torus. The energy eigenvalue $E_{n,\mathbf{k}}$ defines n^{th} energy band disperses with \mathbf{k} in the 1st BZ and all the eigenvalues collectively form a band structure of the system. The gap between two energy bands is called a band gap. The topological properties of these energy bands and the opening and closing of the band gap play a major role in topological insulators.

1. Topology of band structure

Topology concerns quantities that are preserved under continuous deformations of objects. A transformation is “continuous” if it does not cause any sharp cuts or tears in the object. The number of holes (i.e., genus) in a closed surface is an example of a topological invariant. We apply a similar concept in the band structure of the periodic lattice. Let the Hamiltonian depend on some tunable parameters. Varying the parameters, we can continuously deform the band structure of the system. The gapped band structures which can be continuously deformed into one another without closing the gap are topologically equivalent. Such an equivalent class can be characterised by a topologically invariant quantity, the *Chern number*. In the 2D topological insulator, the Chern number of n^{th} band is calculated over the 1st BZ. i.e.,

$$C_n = \frac{1}{2\pi} \iint_{BZ} d^2k \Omega_n(\mathbf{k}) \quad (9)$$

where $\mathbf{A}_n(\mathbf{k}) = i \langle u_{n,\mathbf{k}} | \nabla_{\mathbf{k}} | u_{n,\mathbf{k}} \rangle$ and $\Omega_n(\mathbf{k}) = \nabla_{\mathbf{k}} \times \mathbf{A}_n(\mathbf{k})$. The Chern number always takes an integer value. If Berry curvature $\mathbf{A}_n(\mathbf{k})$ is continuous over the BZ, then the Chern number is zero. One can get that by Using Stokes’s theorem in the Chern number calculation as

$$C_n = \frac{1}{2\pi} \iint_{BZ} d^2k \nabla_{\mathbf{k}} \times \mathbf{A}_n(\mathbf{k}) = \frac{1}{2\pi} \oint_l d\mathbf{k} \cdot \mathbf{A}_n(\mathbf{k}) = 0$$

It is important to note that if the system has time-reversal symmetry (TRS) then $\Omega_n(-\mathbf{k}) = -\Omega_n(\mathbf{k})$, the Chern number, which is an integral of Berry curvature $\Omega_n(-\mathbf{k})$ over the BZ, vanishes. So breaking of time-reversal symmetry leads to a non-trivial Chern number.

A topological phase transition is when the topological invariant quantity of the system changes. this transition happens when the band structure shifts from one equivalence class to another, leading to a change in the Chern number. Consequently, during a topological phase transition, a gap-closing scenario occurs in the band structure. This has significant implications for the formation of edge modes.

2. Edge modes and Bulk edge correspondence

Edge modes are of great interest in the Quantum Hall effect. The gapless edge mode arises in the interface region of two domains of different topological invariance in the bulk. As there is a sudden change in the topological invariant quantity (the Chern number) across the junction, the topological phase transition takes place. During a topological phase transition, a gap-closing scenario occurs in the interface region, leading to the emergence of gapless edge modes that are spatially localized at the interface region. For an electronic system In the case of a TRS-breaking system (e.g., quantum Hall system), the

edge modes are ‘chiral’ i.e., they have distinct propagating directions along the edge. Later we will see that in the case of the quantum Hall system, the edge states have a unidirectional conduction of electrons. It is important to note that the difference between the number of right-moving and left-moving edge states doesnot change. It depends on the topological properties of the bulk states and is equal to the difference between the chern number of the bulk state of the two domains. This is called *Bulk edge correspondence*. Since the system can only change the Chern number through a phase transition when gap closing happens in the band structure, any small change in the band structure in the bulk won’t affect the edge modes. That’s why the chiral edge states are said to be ‘topologically protected’.

III. TOPOLOGICAL INSULATORS IN ELECTRONIC SYASTEM

Before delving into Photonic Topological Insulators (PTIs), it is essential first to understand the basic concepts of topological insulators. These materials exhibit helical edge states that are protected by time-reversal symmetry (TRS). These helical states, form channels that are immune to backscattering or impurities, thus offering robust conduction along the edges.

In this section, we will provide a concise overview of the quantization of the Hall effect and the formation of edge states, focusing on the topological invariant of the QHE, which is given by the Chern number. Following this, we will draw parallels between electronic systems and photonic crystals, highlighting the topological manifestations in both. Without going deeply into mathematics, we will highlight the analogous calculation of the Chern number for Chern PTIs and how it informs our understanding of these systems.

A. Integer quantum hall effect (IQHE)

The integer quantum Hall effect (IQHE) has garnered significant attention over the last few decades. The IQHE was discovered in 1980 by Klaus von Klitzing, who observed quantized Hall conductance in a two-dimensional electron gas subjected to a strong magnetic field at low temperatures. The classical Hall effect is a condensed matter experiment where a transverse potential is observed when a uniform electric field is applied across a thin sample along with a mutually perpendicular magnetic field. The resulting Hall resistivity is given by:

$$\rho_{xy} = \frac{B}{ne} = \frac{1}{\sigma_{xy}}, \quad (10)$$

where ρ_{xy} and σ_{xy} is the off-diagonal component of the resistivity tensor and conductivity tensor respectively, B is the magnetic field and n being the number density of charge carriers. Later, it was observed by von Klitzing

(1980) that at very low temperatures and high magnetic fields, σ_{xy} exhibits plateau-like behaviour with increasing magnetic field. The quantized Hall conductivity is given by:

$$\sigma_{xy} = \frac{e^2}{2\pi\hbar} \nu \quad (11)$$

where $\nu \in \mathbb{Z}$, represents the total number of filled Landau levels. For the IQHE, the Hamiltonian of a 2D electron gas in the presence of a magnetic field in the z-direction is given by

$$H = \frac{(\mathbf{p} + e\mathbf{A})^2}{2m} \quad (12)$$

Taking the Landau gauge choice $\mathbf{A} = xB\hat{y}$ and solving the eigenvalue equation, the energy eigenvalues are:

$$E_n = \hbar\omega_B \left(n + \frac{1}{2} \right), \quad (13)$$

where $\omega_B = \frac{eB}{m}$. The E_n defines the n^{th} Landau level. The explicit wavefunctions depend on two quantum numbers, $n \in \mathbb{N}$ and $k_y \in \mathbb{R}$, and are given by:

$$\psi_{n,k_y}(x, y) \sim e^{ik_y y} H_n(x + k_y l_B^2) e^{-\frac{(x + k_y l_B^2)^2}{2l_B^2}}, \quad (14)$$

where H_n are the Hermite polynomials and $l_B = \sqrt{\hbar/(eB)}$ is the magnetic length. Now, in the presence of an electric field applied in the x -direction, the Hamiltonian can be solved similarly, leading to the energy band:

$$E_{n,k_y} = \hbar\omega_B \left(n + \frac{1}{2} \right) - eEk_y l_B^2 + \frac{e^2 E^2}{2m\omega_B^2}. \quad (15)$$

Comparing the two energy spectra, we see that the degeneracy present in the absence of the electric field is lifted, and the energy now depends on the value of k_y . Because the energy depends on the momentum k_y , it implies that states now drift in the y -direction. The group velocity is proportional to the energy gradient with respect to k_y .

Something special happens at the edge of the 2D sample in a finite sample in a quantum Hall setup. A classical picture would give more intuition. For a fixed magnetic field perpendicular to the sample, all electrons move in a cyclotron orbit in the bulk. Near the edge of the sample, the orbits must collide with the boundary resulting in a skipping motion in which the particles move only in one direction along the one-dimensional boundary. This is the classical picture of the formation of the chiral edge states in the system. (see fig. 2)

1. Topology in IQHE

As discussed before, the topology of the band structure plays a major role in the quantization of Hall conductivity. It is noted that the Chern number corresponds to n^{th}

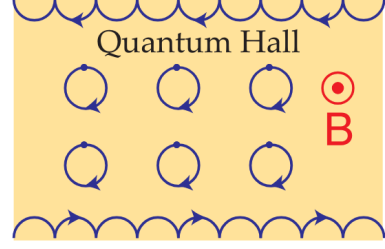


FIG. 2. Figure shows the cyclotron motion of the electron in the bulk of the sample and a skipping orbit motion in the edge in the presence of a perpendicular magnetic field.

Landau level is unity. The origin of the nontrivial Chern number is due to the breaking of the TRS of the system by applying an external magnetic field. Further, the total Chern number, summed over all occupied bands in the Quantum Hall (QH) system is invariant. By TKNN formulation, using the Kubo formula, it is demonstrated that ν in quantized Hall conductivity σ_{xy} is equal to this total Chern number, which is the same as the total number of filled Landau levels.

The edge modes arise when there is a topological phase transition. In the QH system, the edge states arise at the boundary region of the finite sample. Note that vacuum is a trivial insulator i.e. the Chern number vanishes, but the quantum Hall state has a nontrivial Chern number ν . Consequently, the edge states arise due to the topological phase transition across the edge (See fig. 3). The number of edge states is equal to the difference between the Chern number across the edge which is the same as the total Chern number. As the group velocity is proportional to the gradient of energy with respect to k , from the dispersion relation in Fig. 3 it is clear that the edge state has unidirectional group velocity. So the edge modes have chiral property, that is they can propagate only in one direction along the boundary not the opposite direction. Because of the chiral nature of the edge modes, edge currents are immune to backscattering.

B. Quantum Spin Hall Effect

We would like to touch upon the quantum spin hall effect. This is just a brief overview of the workings of this system. It does not include any mathematical framework. It is simply introduced to give the reader an intuitive idea of spin PTIs which would later be touched upon.

Unlike the integer quantum Hall effect (IQHE), where time-reversal symmetry (TRS) is explicitly broken by applying a magnetic field, TRS is preserved in the quantum spin Hall effect (QSHE). The discovery of QSHE materials was motivated by practical challenges associated with QHE, such as the requirement of high magnetic fields and very low temperatures, which limit technological applications.

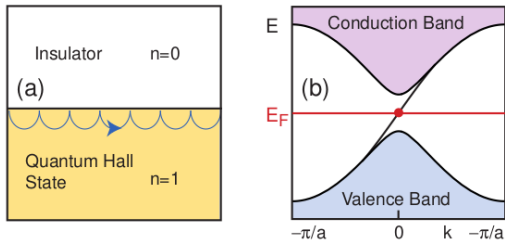


FIG. 3. Figure (a) shows the unidirectional edge state (skipping orbits in the classical picture) in the boundary of the sample. Figure (b) shows the gapless energy dispersion relation contributing to the conduction along the edge. (taken from [1])

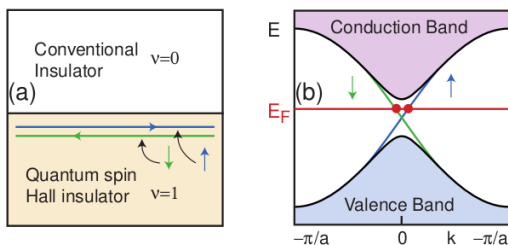


FIG. 4. Figure (a) shows the edge state in the boundary of trivial and nontrivial topological insulators. A pair of counter-propagating channels with opposite spins arise in the edge. (taken from [1])

From the previous discussion, we saw how breaking TRS in QHE leads to a non-zero Chern number, which characterizes the topology of the bulk. However, the preservation of TRS in QSHE means the Chern number is zero, as contributions from spin-up and spin-down states cancel each other out. To capture the non-trivial topology of QSHE systems, another topological invariant, the Z_2 invariant, was introduced.

On the edge, QSHE systems exhibit *helical modes*—pairs of counter-propagating channels with opposite spins, unlike the chiral modes of QHE. These helical modes preserve TRS: a forward-moving spin-up channel is paired with a backwards-moving spin-down channel. Backscattering is suppressed because it would require flipping the spin, which is forbidden by TRS. This robustness makes QSHE systems attractive for exploring topological insulators and potential applications in low-power electronic devices.

IV. PHOTONIC TOPOLOGICAL INSULATORS.

It should not be surprising that many of the quantum topological effects found in condensed-matter systems should find their analogues in photonics. After all,

light is a wave, and the above-mentioned topological effects are merely the consequence of the wave nature of the electrons.

A. Key differences of photonic and electronic systems

The major difference in both systems is the basic constituents of both systems - electrons (fermion) and photons (boson) respectively. Both of them follow different statistics. Electrons are fermions, obeying Fermi-Dirac statistics and the Pauli exclusion principle, which restricts multiple electrons from occupying the same quantum state. This results in the formation of energy bands and dictates electronic behaviours like conductivity and the quantum Hall effect. The occupation of electron states follows the Fermi-Dirac distribution, with a characteristic Fermi level. Photons, on the other hand, are bosons that obey Bose-Einstein statistics. They are not subject to the Pauli exclusion principle, allowing them to accumulate in the same state. This enables phenomena like Bose-Einstein condensation and the formation of coherent light sources (e.g., lasers). In contrast to electrons, photons do not have a chemical potential and can be freely created or annihilated.

Another significant difference is that the topologically nontrivial states arise as the equilibrium state for sufficiently low temperatures, and the electric conductivity is measured under weak or moderate external fields that do not dramatically affect the underlying many-body state. This equilibrium or quasi-equilibrium condition is shared by almost all condensed-matter experiments. Unlike electrons or atoms, photons are not conserved particles—they can be absorbed, scattered, or emitted by the material system. This means maintaining a photon gas requires constant input from an external light source, which makes it hard to achieve stable equilibrium states. Photons can reside in any realistic device only for a finite time and some external driving is needed to inject them into the system. Photon vacuum is physically empty and non-interacting, requiring external intervention for any nontrivial state. In contrast, the electron ‘vacuum’ (filled valence band) is a structured, stable, and intrinsically meaningful state

B. Topology in 2D photonic crystal

In Section II B, we talked about the topology of the 2D electronic crystal. Similarly here drawing parallel with the electronic crystal, we discuss the band formation, Berry phase, Chern number and relevant topics. For the electronic system, we solve the Schrodinger equation, similarly, for the photonic system, our eigenvalue problem is microscopic Maxwell equation. For non-bianisotropic materials with no magnetoelectric coupling, one can eliminate the magnetic field and write Maxwell’s

equation for a field oscillating at frequency ω in the compact form:

$$\nabla \times (\mu^{-1}(\mathbf{r}) \nabla \times \mathbf{E}(\mathbf{r})) = \omega^2 \epsilon(\mathbf{r}) \mathbf{E}(\mathbf{r}). \quad (16)$$

where $\mu(\mathbf{r})$ and $\epsilon(\mathbf{r})$ are the magnetic permeability and dielectric conductivity respectively. For spatially periodic systems where $\mu(\mathbf{r})$ and $\epsilon(\mathbf{r})$ are varying periodically in the system, Bloch's theorem can be applied. These solutions are labelled by the crystal momentum \mathbf{k} and the band index n . The role of the Bloch wavefunction is played here by the electric field $\mathbf{E}_{n,\mathbf{k}}(\mathbf{r})$. Since the equation involves $\epsilon(\mathbf{r})$ multiplying on the right-hand side, we modify the inner product as:

$$\langle \mathbf{E}_1 | \mathbf{E}_2 \rangle = \int d^2\mathbf{r} \sum_{i,j} \mathbf{E}_{1,i}^*(\mathbf{r}) \epsilon_{ij}(\mathbf{r}) \mathbf{E}_{2,j}(\mathbf{r}), \quad (17)$$

where $i, j \in \{x, y, z\}$. Similarly, the Berry connection can be defined as:

$$\begin{aligned} \mathbf{A}_n(\mathbf{k}) &= i \langle \mathbf{E}_{n,\mathbf{k}} | \nabla_{\mathbf{k}} \mathbf{E}_{n,\mathbf{k}} \rangle \\ &= i \int d^2\mathbf{r} \sum_{i,j} \mathbf{E}_{n,\mathbf{k},i}^*(\mathbf{r}) \epsilon_{ij}(\mathbf{r}) \nabla_{\mathbf{k}} \mathbf{E}_{n,\mathbf{k},j}(\mathbf{r}). \end{aligned} \quad (18)$$

Starting from the equation for the Berry connection, the geometrical and topological invariants, such as the Berry curvature and the Chern number, can be calculated in the same way as for electronic systems which is shown before. The Chern number takes non-zero values only when the time-reversal symmetry is broken in the system.

In the context of the quantum hall effect we recall that by introducing a magnetic field the TRS was broken, which led to a non-trivial topology in the bulk. The fundamental constituents i.e. the electrons have an intrinsic charge and hence introduce non-reciprocity in the system. but in the case of photonic systems, the photons have no charge and cannot break the TRS. Gyromagnetic materials introduce off-diagonal terms in the permeability making the tensor anisotropic and directionally dependent and hence breaking the reciprocity/TRS. Gyromagnetic materials consist of a spatially periodic arrangement of material elements, giving spatially periodic dielectric permittivity $\epsilon_{ij}(\mathbf{r})$ and magnetic permeability $\mu_{ij}(\mathbf{r})$ tensors. In such a geometry, one can apply to photons the Bloch theorem originally developed in solid-state physics for electrons in crystalline solids. Photon states organize themselves into allowed bands separated by forbidden gaps and are labelled by their wave vector defined within the first Brillouin zone of the periodic lattice.

V. EXPERIMENTAL OBSERVATIONS AND REALIZATIONS

It was Raghu and Haldane (2008, [6]) who initially put forward the idea of chiral edge states in photonic systems. They theoretically predicted the existence of

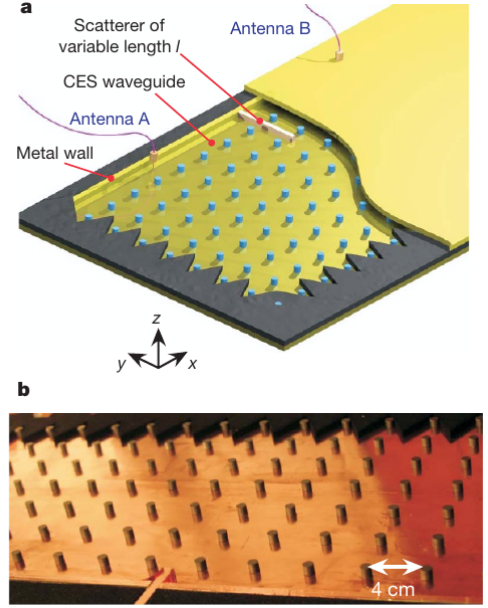


FIG. 5. Figure shows the structure of the photonic crystal used as Chern PTI in the experiment by Wang et al [7].

these modes. It was later that Wang et al (2008) experimentally realized the existence of the chiral edge states (CES). Here, we discuss briefly about the experiment by Wang et al.

The experimental system shown in Fig 5 involves a gyromagnetic, 2D-periodic photonic crystal consisting of a square lattice of ferrite rods composed of vanadium-doped calcium-iron-garnet in air bounded on one side by a non-magnetic metallic cladding. The interface between the photonic crystal and the cladding acts as a confining edge or waveguide for CESs. The structure is sandwiched between two parallel copper plates (yellow) for confinement in the z direction and surrounded with microwave-absorbing foams (grey regions). Two dipole antennas, A and B serve as feeds and/or probes for the vector network analyzer. A variable-length (l) metal obstacle (orange) with a height equal to that of the waveguide (7.0 mm) is inserted between the antennas to study scattering. A 0.20T D.C. magnetic field is applied along the z direction using an electromagnet.

To get a nontrivial Chern number, the time-reversal symmetry has to be broken in the system. It is noted that the doped ferrite rods used in the experiment have the gyromagnetic property. An external magnetic field introduces anisotropy in the magnetic permeability of the ferrite rod of the form

$$\mu_{ij}(\mathbf{r}) = \begin{pmatrix} \mu_0 & -i\kappa & 0 \\ i\kappa & \mu_0 & 0 \\ 0 & 0 & \mu_z \end{pmatrix}.$$

Here off-diagonal terms depend on κ which captures the effect of the magnetic field and is nonzero only in the presence of the external magnetic field. The presence of

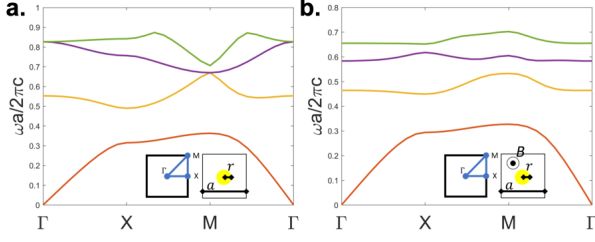


FIG. 6. Figure shows the numerical simulation of the photonic bands of the system in Wang et al experiment. In (a), there is degeneracy at Γ and M in the band structure and in (b) the band gap arises in those points. (taken from [4])

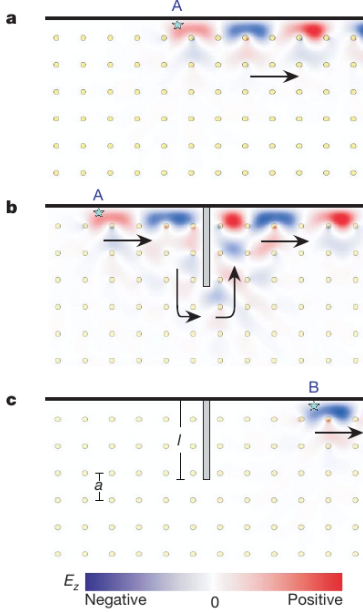


FIG. 7. The figure (a) shows the chiral edge state of the PTI. Figure (b) and (c) shows the propagation of chiral edge state when conducting barrier is placed in the waveguide. (taken from [7])

an external magnetic field breaks the TRS of the system, leading to a nonzero Chern number.

After performing numerical simulations of the above-said system they found that a gap opens between the second and third transverse magnetic (TM) bands (see fig 6). the second and third bands of this photonic crystal acquire Chern numbers of 1 and -2 respectively. Because the sum of the Chern numbers over the first and second bands is 1, exactly one CES is predicted to exist at the interface between the photonic crystal and the metal cladding.

The band gaps and the CES waveguide were characterized using a two-port vector network analysis using a pair of dipole antennas labelled A and B. At frequencies within the second band gap, it was observed a strong forward transmission, approximately 50 dB greater than the backward transmission at mid-gap frequencies as shown

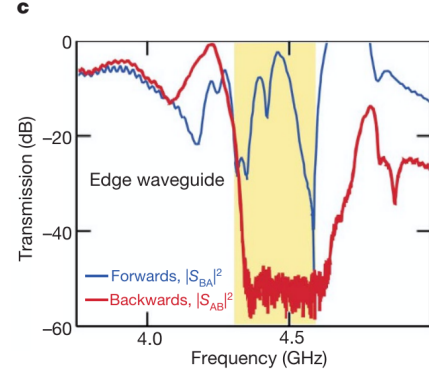


FIG. 8. Figure shows the magnitudes of forward and backward transmission of CES displayed by the VNA. (taken from [7])

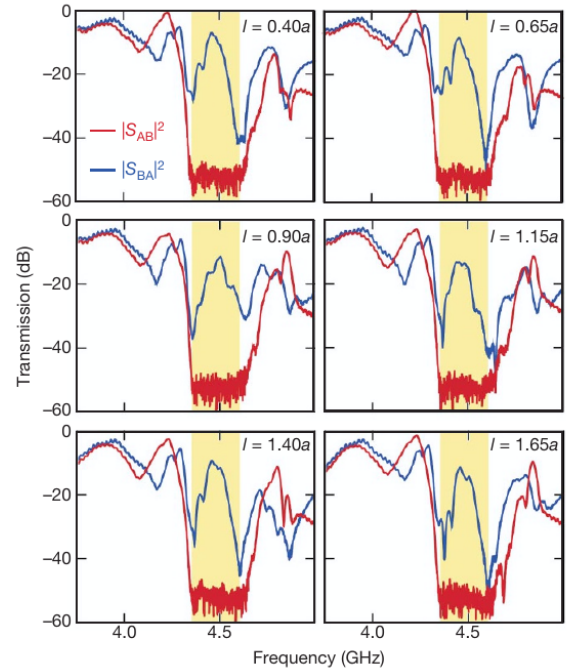


FIG. 9. Figure shows the magnitudes of forward and backward transmission of CES when a conducting obstacle is placed in the waveguide. (taken from [7])

in Fig8. Over much of this frequency range, the backward transmission was below the noise floor of the network analyser, which suggests an even greater actual contrast. This confirms that backwards-propagating modes are highly evanescent, as predicted. They also tested the robustness of the unidirectional propagation by studying the effect of a large obstacle on transmission. They gradually inserted a conducting barrier across the waveguide, blocking the direct path between antennas A and B. The measured transmission behaviour at different stages of the insertion Fig9 remains basically

the same as that in Fig8 the transmission between 4.35 and 4.62 GHz remains strongly non-reciprocal, with a 40–50-dB difference between the forward and backward transmissions. This finding agrees with the theoretical prediction that power transmission by means of CESs is fundamentally insensitive to scattering from arbitrarily large defects (Fig. 2b).

VI. CONCLUSION AND OUTLOOK

In this paper, we have introduced photonic topological insulators (PTIs) by drawing parallels with the well-known quantum Hall effect (QHE) and explored the role of topology in governing their unique properties. The focus was on understanding how PTIs leverage principles from condensed matter physics, such as topological invariants like the Chern number, and adapt them to photonic systems through innovative approaches like breaking time-reversal symmetry using gyromagnetic materials.

Although the paper was mainly focused on chern PTIs, there is a different class of PTIs known as the spin PTIs. Spin Photonic Topological Insulators (Spin PTIs) are a class of photonic systems that mimic the behaviour of

the quantum spin Hall effect (QSHE) seen in electronic systems. In photonics, the role of spin is replaced by other degrees of freedom such as circular polarization or modes within photonic crystals. Spin PTIs retain TRS. The edge states in Spin PTIs are doubly degenerate but counter-propagating, just like in QSHE.

Due to the robustness of the edge states. The applications of PTIs are vast. They improve signal integrity in telecommunications, ensuring minimal losses even around bends or through imperfections in waveguides. Chern and Spin PTIs provide platforms for fault-tolerant quantum information processing. They could be used in topological quantum computing schemes that require robust manipulation of quantum states. PTIs are being utilized to create topological lasers that exploit edge states for robust lasing action.

ACKNOWLEDGMENTS

I would like to express my sincere gratitude to Prof. Nirmalaya Ghosh, whose invaluable guidance, insights, and support have greatly contributed to the completion of this work. I am also thankful to the Institute for providing the resources and facilities needed for this research.

-
- [1] Hasan, M. Z., & Kane, C. L. (2010). *Colloquium: Topological insulators*. Reviews of Modern Physics, 82(4), 3045–3067. doi:10.1103/revmodphys.82.3045
 - [2] Ozawa, T., Price, H. M., Amo, A., Goldman, N., Hafezi, M., Lu, L., ... Carusotto, I. (2019). *Topological photonics*. Reviews of Modern Physics, 91(1). doi:10.1103/revmodphys.91.015006
 - [3] Lu, L., Joannopoulos, J. & Soljačić, M. *Topological photonics*. Nature Photon 8, 821–829 (2014). <https://doi.org/10.1038/nphoton.2014.248>
 - [4] Bisharat, D., Davis, R., Zhou, Y., Bandaru, P., & Sievenpiper, D. (2021). *Photonic Topological Insulators: A Beginner's Introduction [Electromagnetic Perspectives]*. IEEE Antennas and Propagation Magazine, 63(3), 112–124. doi:10.1109/map.2021.3069276
 - [5] Garg, A. (2010). *Berry phases near degeneracies: Beyond the simplest case*. American Journal of Physics, 78(7), 661–670. doi:10.1119/1.3377135
 - [6] Raghu, S., & Haldane, F. D. M. (2008). *Analogs of quantum-Hall-effect edge states in photonic crystals*. Physical Review A, 78(3). doi:10.1103/physreva.78.033834
 - [7] Wang, Z., Chong, Y. D., Joannopoulos, J. D., & Soljačić, M. (2008). *Reflection-Free One-Way Edge Modes in a Gyromagnetic Photonic Crystal*. Physical Review Letters, 100(1). doi:10.1103/physrevlett.100.013905